generate the intriguing intermediate $Cp^*_2Ir_2(\mu\text{-}O)$ or bimolecular pathways in which the incoming phosphine adds either to the metal center to which PPh_3 is bound or to the remote center to give an intermediate or transition state $Cp^*(L)Ir(\mu\text{-}O)Ir(L')Cp^*$.

The most dramatic transformation of the phosphine μ-oxo complexes **6a,b** occurs upon heating them in benzene or toluene solution without added reagents. This leads to new materials (**7a** and **7b**) which have been formed by deep-seated rearrangement. In the case of **6a**, the product is formed after 45 min at 85 °C in 85% isolated yield; **6b** is converted more readily, forming a 31% isolated yield in 2 days at 25 °C (both are isolated as golden yellow solids). The appearance of strong IR bands (3507 cm^{-1} for **7a**; 3525 cm^{-1} for **7b**) indicated the presence of an O–H group in each molecule. Further evidence for an O–H group includes a high field ^1H NMR resonance (δ −3.43 ppm in C_6D_6 for **7a**: d, J_{HP} = 13.8 Hz; −3.48 for **7b**: d, J_{HP} = 13.5 Hz), which disappears upon addition of D_2O. In combination with ^1H and ^{13}C NMR spectra, these data suggested the structure shown in Scheme I for the rearranged products. In support of this formulation, complex **7a** has been degraded with HCl in toluene-d_8 to give benzene (identified by ^1H NMR and GC/MS) and $Cp^*Ir(HPPh_2)Cl_2$ (**8a**,[3] identified by ^1H and ^{31}P NMR) as the major identifiable products. Degradation of the analogous complex **7b** in C_6D_6 similarly yields toluene (identified by ^1H NMR and GC/MS) and $Cp^*Ir(HPTol_2)Cl_2$ (**8b**, identified by ^1H [δ 1.31 (d, J = 2.3, Cp^*)] and ^{31}P NMR [δ −12.3 (d, J = 407.5)]). The structure of **7a** has been confirmed by X-ray diffraction; an ORTEP diagram is included in Scheme I, and details are provided as Supplementary Material.[13]

In recent years much attention has been directed toward the possible role of reactive transition-metal oxo complexes as oxidizing and oxygen-atom-transfer agents.[14] However, there have been very few reports of isolable oxo complexes of the noble metals[2b,15] (especially those noted for undergoing rapid C–H insertion reactions) because the M–O bond is generally stabilized by highly oxidized and electron-deficient metal centers.[14] Although late transition metals have been shown to cleave P-aryl bonds to form benzyne complexes,[16,17] the transfer of the H atom from a C–H bond to an oxygen atom receptor in the conversion of **6** to **7** is, to our knowledge, so far unique to this system. It is our hope that the successful construction of additional low-valent, electron-rich transition-metal oxo species, which exhibit enhanced reactivity at both the metal and oxygen sites, will assist in the development of materials useful in the oxygenation of traditionally inert organic molecules.[18]

Acknowledgment. We are grateful for financial support of this work from the National Science Foundation (CHE-8722801). T.F. acknowledges a fellowship from the NSF. We are also grateful to the Johnson-Matthey Corp. for a generous loan of iridium chloride and to Prof. Paul R. Sharp (University of Missouri, Columbia) for helpful discussions and for disclosing results prior to publication.

Supplementary Material Available: Spectroscopic and analytical data for complexes **2**, **3**, **4**, **5a,b**, **6a,c**, **7a,b**, and **8a**, and details of the structure determination of complexes **6a** and **7a** including experimental description, ORTEP drawings showing full atomic numbering scheme, crystal and data collection parameters, anisotropic thermal parameters (B's), positional parameters and their estimated standard deviations, and intramolecular distances and angles (46 pages); tables of calculated and observed structure factors for **6a** and **7a** (47 pages). Ordering information is given on any current masthead page.

(13) The structure was solved by Patterson methods and refined by standard least-squares and Fourier techniques. Crystal data for **7a** at 25 °C: space group *Pcbm*; a = 8.7305 (9) Å, b = 20.8495 (13) Å, c = 21.9477 (19) Å, $\alpha = \beta = \gamma = 90.0°$; V = 3995.1 (10) Å^3; Z = 4; d_c = 1.70 g cm^{-0}; μ_{calcd} = 67.0 cm^{-1}; R = 2.26%, wR = 3.06%, GOF = 1.54, n_{var} = 236, n_{obsd} = 2026.

(14) For a review on metal-centered oxygen-atom-transfer reactions, see: Holm, R. H. *Chem. Rev.* **1987**, *87*, 1401.

(15) (a) Carty, P.; Walker, A.; Mathew, M.; Palenik, G. J. *J. Chem. Soc., Chem. Commun.* **1969**, 1374. (b) Brownlee, G. S.; Carty, P.; Cash, D. N.; Walker, A. *Inorg. Chem.* **1975**, *14*, 323. (c) Cheng, P.-T.; Nyburg, S. C. *Inorg. Chem.* **1975**, *14*, 327.

(16) Brown, S. C.; Evans, J.; Smart, L. E. *J. Chem. Soc., Chem. Commun.* **1980**, 1021.

(17) For a review on transition-metal-mediated phosphorus–carbon bond cleavage reactions, see: Garrou, P. E. *Chem. Rev.* **1985**, *85*, 171.

(18) For reviews of C–H activation, see: (a) Shilov, A. E. *Activation of Saturated Hydrocarbons by Transition Metal Complexes*; D. Riedel Publishing Co.; Dordrecht, 1984. (b) Crabtree, R. H. *Chem. Rev.* **1985**, *85*, 245.

Tubular Silicate-Layered Silicate Intercalation Compounds: A New Family of Pillared Clays

Ivy D. Johnson, Todd A. Werpy, and Thomas J. Pinnavaia*

Department of Chemistry and Center for Fundamental Materials Research Michigan State University East Lansing, Michigan 48824

Received May 22, 1988

Metal oxide pillared clays[1-9] are among the most promising microporous materials to be developed since the advent of synthetic zeolites more than four decades ago. Interest in these materials is stimulated in part by their properties as heterogeneous catalysts, especially for the shape-selective cracking of petroleum to high-energy fuels.[10-12] These materials normally are prepared by intercalative ion exchange of smectite clays with polyoxocations, followed by thermal conversion of the intercalated ion to metal oxide aggregates of molecular dimension.

Several workers have recognized the possibility of directly intercalating metal oxide sol particles into clay galleries.[13-16] However, the formation from sols of pillared clay derivatives with *uniform* gallery heights presupposes the existence of pillaring particles of rigorously uniform size and shape. Although nonaggregated sols in the submicron range are routinely available, those with sizes approaching molecular dimension (<50 Å) are difficult to produce in monodispersed form.

We have found that a sol containing the tubular metal oxide imogolite[17-20] can be directly intercalated as a regular monolayer in the galleries of smectite clays. These novel intercalates, schematically shown in Figure 1, are regular tubular silicate-layered silicate (TSLS) nanocomposites that constitute a new

(1) Vaughan, D. E. W.; Lussier, R. J. *Preprints 5th International Conference on Zeolites*; Naples, Italy, June 2–6, 1980.
(2) Pinnavaia, T. J. *Science* **1983**, *220*, 365.
(3) Lahav, N.; Shani, V.; Shabtai, J. *Clays Clay Miner.* **1978**, *26*, 107.
(4) Loeppert, R. H., Jr.; Mortland, M. M.; Pinnavaia, T. J. *Clays Clay Miner.* **1979**, *27*, 201.
(5) Yamanaka, S.; Brindley, G. W. *Clays Clay Miner.* **1979**, *27*, 119.
(6) Sterte, J.; Otterstedt, J. *Applied Cat.* **1988**, *38*, 131.
(7) Adams, J. M. *Applied Clay Science* **1987**, *2*, 309.
(8) Tilak, D.; Tennkoon, B.; Jones, W.; Thomas, J. M. *J. Chem. Soc., Faraday Trans.* **1986**, *82*, 3081.
(9) Barrer, R. M. Zeolites and Clay Minerals as Sorbents and Molecular Sieves. Academic Press: New York, 1978.
(10) Shabtai, J.; Lazar, R.; Oblad, A. G. *Stud. Surf. Sci. Catal.* **1981**, *7*, 828.
(11) Occelli, M. L. *Ind. Eng. Chem. Prod. Res. Dev.* **1983**, *22*, 253.
(12) Lussier, R. J.; Magee, J. S.; Vaughan, D. E. W. *Preprints 7th Canadian Symposium on Catalysis*; Edmonton, Alberta, Canada, October 19–22, 1980.
(13) Occelli, M. L. *Proceedings of the International Clay Conference*; Denver, CO, July 28–August 2, 1985, 319.
(14) Yamanaka, S.; Nishihana, T.; Okumera, F.; Hattori, M. *Abstracts of Papers*, 24th Meeting of the Clay Mineral Society 1987.
(15) Moini, A.; Pinnavaia, T. J. *Solid State Ionics* **1988**, *26*, 119.
(16) Occelli, M. L. *J. Mol. Catal.* **1986**, *35*, 377.
(17) Yoshinaga, N.; Aomine, S. *Soil Plant Nutr.* **1962**, *8*, 6.
(18) Farmer, V. C.; Fraser, A. R. *J. Chem. Soc., Chem. Commun.* **1977**, *13*, 462.
(19) Farmer, V. C.; Adams, M. J.; Fraser, A. R.; Palmieri, F. *Clay Miner.* **1983**, *18*, 459.
(20) van der Gaast, S. J.; Wada, K.; Wada, S.-I.; Kukuto, Y. *Clays Clay Miner.* **1985**, *33*, 237.

0002-7863/88/1510-8545$01.50/0

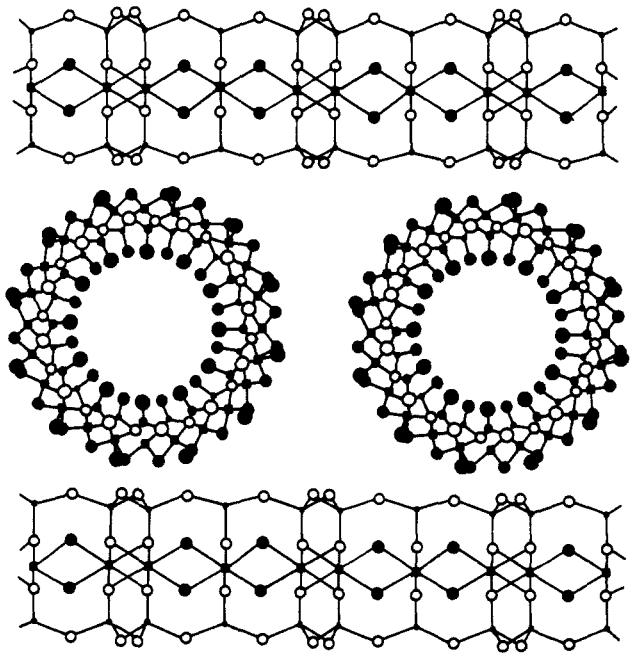

Figure 1. Schematic illustration of the tubular silicate-layered silicate (TSLS) intercalation complex formed between imogolite and Na^+ montmorillonite. The Na^+ exchange ions which co-occupy the gallery surfaces of the montmorillonite are not shown. Other smectite clays (e.g., hectorite and fluorohectorite) may be substituted for montmorillonite as the host clay. Legend: oxygen, open circles; silicon, smaller filled circles; hydroxyls, larger filled circles; aluminum, filled squares. The difference in atom sizes for the imogolite tube is intended to provide some depth-of-field perspective.

family of pillared clay materials.

The structure of imogolite can be viewed as a gibbsite sheet, 11–12 edge-shared octahedra in width, which has closed on itself to form a tube. Orthosilicate tetrahedra are condensed to the inner hydroxyl plane at triangular faces above vacant octahedral positions. The outside tube diameter is ~23 Å, and the tube length varies in the range 10^2–10^5 Å. The internal channel (~8.2 Å) normally is occupied by water. The chemical composition, written in order of outer to inner atomic planes, is $(HO)_3Al_2O_3Si(OH)$.

The synthesis of an aqueous imogolite suspension (0.9 wt %) was achieved by the hydrolysis of $Al(\sigma\text{-}BuO)_3$ and $Si(OEt)_4$ according to the method of Farmer.[21] A dialyzed portion of the suspension exhibited a Si/Al molar ratio (0.53 ± 0.08), in accord with the expected value of 0.50. A Na^+-montmorillonite clay suspension (0.9 wt %) was added to the imogolite suspension in a ratio of 1:2 (v/v). The product was centrifuged and washed with distilled water until the wash solution was free of excess imogolite. The absence of imogolite in the wash solution was indicated by the lack of gel formation upon addition of 0.1 M NH_4OH. The final TSLS product was then dried in air at room temperature.

Oriented film samples prepared by evaporation of 1 wt % suspension of the TSLS complex onto a glass slide exhibited three orders of 00*l* reflection. A plot of $4\pi \sin \theta/\lambda$ vs l gave a slope corresponding to a basal spacing of 34.0 ± 1.0 Å. This value is in accord with the van der Waals' thickness of an imogolite tube (23 Å) and the thickness of a montmorillonite sheet (9.6 Å). The ^{29}Si MAS-NMR spectrum of the complex exhibited resonances at −79.3 and −93.5 ppm indicative, respectively, of the orthosilicate Q^0 site in imogolite[22] and the Q^3 environment in montmorillonite in which there are three Si–O linkages to each Si.[23-25] These

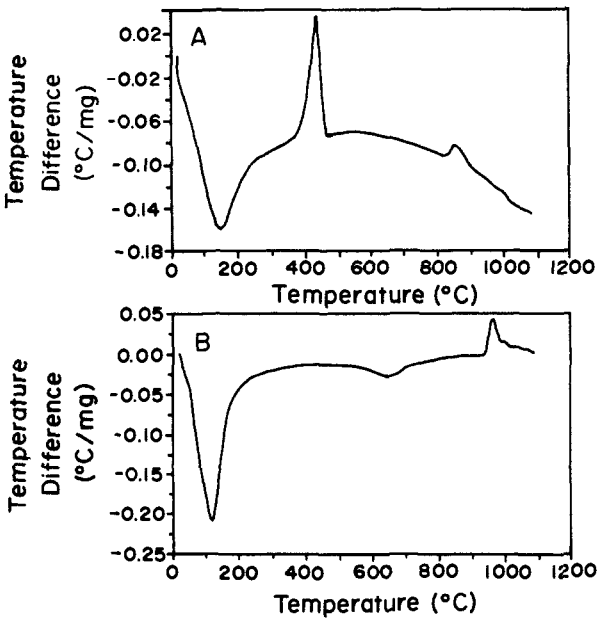

Figure 2. Differential thermal analysis curves for (A) imogolite and (B) imogolite–montmorillonite TSLS intercalation complex.

results are consistent with the model proposed in Figure 1, wherein the imogolite intercalates as a monolayer into montmorillonite with little or no change in chemical constitution or structure. TSLS complexes with similar properties were also obtained with other smectite-layered silicates as the host species (e.g., fluorohectorite and hectorite).

The mode of interaction between the imogolite tube surfaces and the gallery surfaces of the clay most likely involves hydrogen bonding. Electrostatic interactions are also possible because the isoelectric point of imogolite (pH < 9.0)[6,19,26] is sufficiently large to allow the tubes to carry a net positive charge under the synthesis conditions employed. However, the extent to which the clay layer charge is compensated by the pillaring imogolite tubes is relatively low. The TSLS complex formed with montmorillonite exhibits a cation exchange capacity of 44.5 mequiv/100 g,[27] a value consistent with an intercalate containing approximately equal amounts of tubular and layered silicate components.

Differential thermal analyses studies indicate that imogolite is dramatically stabilized by intercalation. Pure imogolite (Figure 2A) exhibits a dehydration endotherm (<200 °C), a dehydroxylation exotherm (>350 °C), and a recrystallization exotherm (800 °C). The dehydroxylation process is accompanied by the collapse of the tubes and the formation of siloxane bonds, as judged from the appearance of a strong IR Si–O–Si stretching frequency (1090 cm^{-1}) and the loss of the orthosilicate band at 995 cm^{-1}. In contrast, the TSLS complex (Figure 2B) exhibits a dehydration endotherm (<200 °C), an endotherm due to montmorillonite dehydroxylation (>500 °C), and a recrystallization exotherm (>900 °C). However, no imogolite dehydroxylation exotherm is observed for the TSLS complex, and the 34 Å basal spacing is retained even at 400 °C.

We tentatively propose that imogolite stabilization in the intercalated state is due in part to packing factors which minimize tube distortions. Additional stabilization may result from H-bonding interactions between the tube surface and the gallery surfaces of the layered silicate host. Our monolayer model for the imogolite–montmorillonite complex places the imogolite tubes in van der Waals contact within the layered silicate galleries. The tubes, which are almost certainly of variable length, may be clustered into domains. The gallery surfaces between domains

(21) Farmer, V. C. U.S. Patent 4,252,779, 1981.
(22) Barron, P. F.; Wilson, M. A.; Campbell, A. S.; Frost, R. L. *Nature* **1982**, *299*, 616.
(23) Goodman, B. A.; Russell, J. D.; Montez, B.; Oldfield, E.; Kirkpatrick, R. J. *Phys. Chem. Miner.* **1985**, *12*, 342.
(24) Oldfield, E.; Kinsey, R. A.; Smith, K. A.; Nichols, J. A.; Kirkpatrick, R. J. *J. Magn. Reson.* **1983**, *51*, 325.
(25) A weak resonance at −109 ppm was also present due to a small silica impurity in the montmorillonite.
(26) Horikawa, Y. *Clay Sci.* **1975**, *4*, 255.
(27) The cation exchange capacity was determined by the NH_4^+ exchange method: Busenberg, E.; Clemency, C. V. *Clays Clay Miner.* **1973**, *21*, 213.

would then be available for adsorption of guest molecules. In addition, the internal surfaces of the intercalated imogolite tubes represent a second type of surface for guest molecule adsorption.

The presence of regular microporosity for the montmorillonite complex was indicated by Langmuir-type adsorption isotherms for adsorbates with kinetic diameters (<8.6 Å). The pore volume observed for water as an adsorbate (2.65 Å kinetic diameter) was 0.14 cm^3/g. Nitrogen (3.64 Å) and benzene (5.84 Å) both gave a pore volume of 0.094 ± 0.02 cm^3/g. With 1,3,5-triethylbenzene (8.6 Å) and perfluorotributylamine (10.2 Å) as the adsorbates, the pore volume was reduced to <0.014 cm^3/g. Since these latter adsorbates are not expected to access the internal channel of the intercalated imogolite, we conclude that the internal surfaces of the tubular silicate contribute substantially to the zeolitic microporosity observed for adsorbates with a kinetic diameter <8.6 Å.

The BET-N_2 surface area for the montmorillonite TSLS was measured as a function of outgassing temperature. For temperatures in the range 125–435 °C, the surface area was 295 ± 15 m^2/g. Outgassing at 500 °C resulted in a reduction in surface area to a value of 92 m^2/g. The loss in surface area was accompanied by the loss of the −79.3 ppm imogolite resonance in the ^{29}Si MAS NMR spectrum and the appearance of an amorphous silica peak at −108 ppm. Thus, the thermal stability of the TSLS complex appears to be determined by the dissociation of the imogolite tubes.

We anticipate that TSLS complexes will be useful for selective absorption and catalysis. The potential of this new family of pillared clays for acid catalysis is suggested by preliminary studies of alcohol dehydration. Ethanol, isopropyl alcohol, and *tert*-butyl alcohol all undergo dehydration over TSLS complexes at temperatures in the range 200–300 °C to afford corresponding olefins.

Acknowledgment. The support of this research by the National Science Foundation through Grant DMR-8514154 and by the Michigan State University Center for Fundamental Materials Research is gratefully acknowledged.

Assignment of a New Conformation-Sensitive UV Resonance Raman Band in Peptides and Proteins

Sunho Song and Sanford A. Asher*

Department of Chemistry, University of Pittsburgh Pittsburgh, Pennsylvania 15260

Samuel Krimm and Jagdeesh Bandekar

Biophysics Research Division, University of Michigan, Ann Arbor, Michigan 48109

Received July 14, 1988

Preresonance Raman specta of *N*-methylacetamide (NMA)[1,2] and polypeptides[2,3] and UV resonance Raman spectra of NMA[4,5] and proteins[6-8] have shown the presence of a band (or bands), generally near 1400 cm^{-1} but in fact varying from 1496 cm^{-1} in NMA[4] to below 1350 cm^{-1} in α-helical poly(L-lysine) (PLL),[2] whose assignment and significance are unclear. Because this band in ionized PLL (at 1391 cm^{-1}) disappears in D_2O solution,[2] it was "tentatively assigned to a coupled vibration of the —NH—CH—CO— group".[2] Other authors have assigned it to the CH_3 antisymmetric bend[1,4] or to the photoinduced cis peptide group[9] in NMA, to the COO^- symmetric stretch in ionized poly(L-glutamic acid) (PGA)[2] and tropomyosin,[8] and to the CH_2 wag or twist in PLL[3] as well as to the CH_2 bend in cytochrome *c*.[7] Experimental studies on NMA (presented here) and on small peptides as well as PGA and PLL,[10] together with a theoretical analysis of the conformational dependence of this band,[11] indicate that it derives from the overtone of amide V (CN torsion plus NH out-of-plane bend). The amide V band, which is normally strong in the infrared but very weak in the Raman spectrum, is sensitive to the polypeptide chain conformation. Thus, the frequency and intensity of this overtone band can be used as a new sensitive probe of secondary structure in proteins.

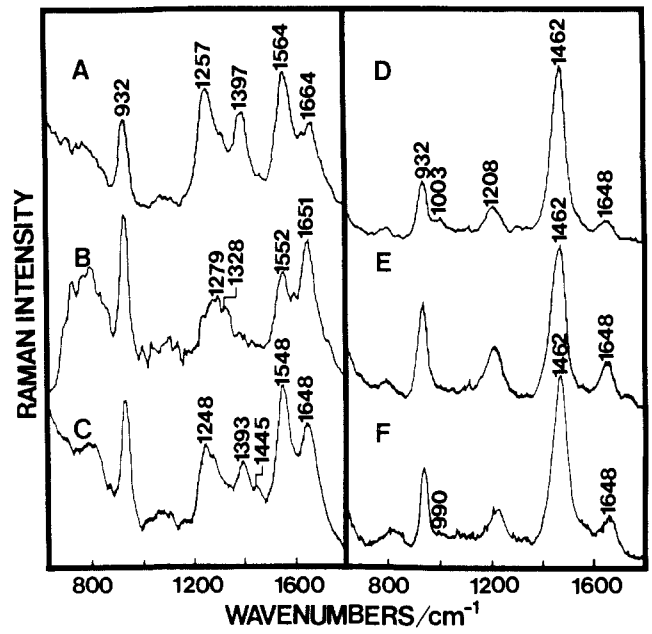

Figure 1. Raman spectra of poly(L-glutamic acid) (0.11 mM) at 218-nm excitation: (A) random coil, (B) α-helix and (C) β-sheet in water, (D) random coil, (E) α-helix and (F) β-sheet in D_2O. A 932-cm^{-1} band is the symmetric stretch of ClO_4^- (0.2 M) used as an internal intensity standard.

The conformation- and deuteriation-dependence of this band in PGA[10] are shown in Figure 1 for 218-nm excitation. The amide I, II, and III modes are located near 1650, 1550, and 1250 cm^{-1}, respectively, and shift or disappear as expected[10,12] on N-deuteriation. The 932-cm^{-1} band is the symmetric stretch mode of ClO_4^-, used as an internal intensity standard.[13] The putative amide V overtone bands are found at 1397 cm^{-1} in ionized PGA (Figure 1A), near 1330 cm^{-1} in α-PGA (Figure 1B), and at 1445 and 1393 cm^{-1} in β-PGA (Figure 1C). Their disappearance on deuteriation (the 1462-cm^{-1} band is amide II′ and the 1208-cm^{-1} band is due to D_2O) indicates that the mode involved must have an NH component. An assignment to a COO^- mode is excluded by its absence in the deuteriated species, by its Albrecht A-term preresonant state of 194–201 nm,[4,10] corresponding to the amide $\pi \rightarrow \pi^*$ electronic transition, and by its very high cross section compared to that found for COO^- in acetate ion;[11] the fact that strong bands near 1400 cm^{-1} in *normal* Raman spectra of molecules containing COO^- are properly assignable to the COO^-

(1) Harada, I.; Sugawara, Y.; Matsuura, H.; Shimanouchi, T. *J. Raman Spectrosc.* **1975**, *4*, 91–98.
(2) Sugawara, Y.; Harada, I.; Matsuura, H.; Shimanouchi, T. *Biopolymers* **1978**, *17*, 1405–1421.
(3) Chinsky, L.; Jolles, B.; Laigle, A.; Turpin, P. Y. *J. Raman Spectrosc.* **1985**, *16*, 235–241.
(4) Dudik, J. M.; Johnson, C. R.; Asher, S. A. *J. Phys. Chem.* **1985**, *89*, 3805–3814.
(5) Mayne, L. C.; Ziegler, L. D.; Hudson, B. *J. Phys. Chem.* **1985**, *89*, 3395–3398.
(6) Rava, R. P.; Spiro, T. G. *Biochemistry* **1985**, *24*, 1861–1865.
(7) Copeland, R. A.; Spiro, T. G. *Biochemistry* **1985**, *24*, 4960–4968.
(8) Copeland, R. A.; Spiro, T. G. *J. Am. Chem. Soc.* **1986**, *108*, 1281–1285.
(9) Harada, I.; Takeuchi, H. *Spectroscopy of Biological Systems*; Clark, R. J. H., Hester, R. E., Eds.; Wiley: New York, 1986; pp 113–175.
(10) Song, S.; Asher, S. A. Submitted for publication in *J. Am. Chem. Soc.*, 1988.
(11) Krimm, S.; Song, S.; Asher, S. A. Submitted for publication in *J. Am. Chem. Soc.*, 1988.
(12) Krimm, S.; Bandekar, J. *Adv. Protein Chem.* **1986**, *38*, 181–364.
(13) Dudik, J. M.; Johnson, C. R.; Asher, S. A. *J. Chem. Phys.* **1985**, *82*, 1732–1740.

0002-7863/88/1510-8547$01.50/0